Journal of Alloys and Compounds 499 (2010) 187–193

Contents lists available at ScienceDirect

Journal of Alloys and Compounds

journal homepage: www.elsevier.com/locate/jallcom

Structural, optical and microscopic studies of tungsten substituted molybdenum diselenide thin films

D.J. Sathe [d,*], P.P. Hankare [a], A.H. Manikshete [b], P.A. Chate [c], A.A. Patil [a]

[a] Solid State Research Laboratory, Dept. of Chemistry, Shivaji University, Kolhapur, MS, India
[b] Dept. of Chemistry, Walchand college, Solapur, MS, India
[c] Dept. of Chemistry, J.S.M. College, Alibag, MS, India
[d] Dept. of Chemistry, KIT's College of Engineering, Kolhapur, MS, India

ARTICLE INFO

Article history:
Received 10 August 2009
Received in revised form 13 March 2010
Accepted 18 March 2010
Available online 23 March 2010

Keywords:
Thin films
Semiconductors
Chemical synthesis
X-ray diffraction

ABSTRACT

A modified chemical bath deposition method has been developed to prepare $Mo_{1-x}W_xSe_2$ layer type semiconductor thin films. Various preparative conditions of the thin films are outlined. The films were characterized by X-ray diffraction, optical absorption, electrical measurements and thermoelectric techniques. The grown films were found to be uniform, well adherent to substrate and brown in color. The X-ray diffraction (XRD) study indicates the polycrystalline nature in single hexagonal phase over whole range of composition. Analysis of absorption spectra gave direct type of band gap, the magnitude of which increases slightly as tungsten content in the film is increased and electrical conductivity at room temperature was found to be 10^{-5} to 10^{-2} $(\Omega\,cm)^{-1}$. All the films show n-type conductivity.

1. Introduction

The transition metal dichalcogenides ($MoSe_2$, WSe_2, MoS_2, and WS_2) have layered structure and attracted many researchers due to their interesting properties like superconductivity, charge density waves, intercalation compound formation etc. Most of the TMDC compounds studied can be considered structurally as strongly bonded two-dimensional X–M–X (M = metal, X = chalcogen) layers loosely coupled to one another by relatively weak van der Waals type forces [1–4]. Recent investigations have shown that the layered type semiconducting group VI transition metal dichalcogenides, which absorb visible and near-IR light are particularly interesting materials for photoelectrochemical solar energy conversion. Recent applications include intercalation compounds, long-life PEC solar cells, catalysis in hydro treating processes high temperature- high pressure solid lubricants, and rechargeable batteries [5–11]. Agarwal et al. described the growth and some of the key properties of $Mo_{1-x}W_xSe_2$, WS_xSe_{2-x}, $MoSe_xTe_{2-x}$ and $Mo_{0.5}W_{0.5}Se_2$ single crystals [12–16]. Similar mixed crystals of compounds such as $Mo_{0.02}W_{0.98}Se_2$, $Mo_{0.5}W_{0.5}Se_2$ and $Mo_xW_{1-x}Se_2$ by using various methods have been published earlier [17,18,21].

In the present investigation we describe synthesis of $Mo_{1-x}W_xSe_2$ thin films grown on glass substrates by chemical method. Structural, morphological, optical, and electrical properties of sample were study and reported.

2. Experimental details

All the solutions were exclusively prepared in double-distilled water and the basic chemicals used were of AR grade. All the solutions were kept in air tight bottles. It contains ammonium molybdate, sodium tungestate, tartaric acid, hydrazine hydrate, sodium sulphite and selenium powder. Sodium selenosulphate was prepared by following the reported method [19].

The deposition of typical $Mo_{0.5}W_{0.5}Se_2$ thin films was made in a reactive solution obtained by mixing 5 mL (0.2 M) ammonium molybdate, 5 mL (0.2 M) sodium tungestate, 5 mL (1 M) tartaric acid, 20 mL (10%) hydrazine hydrate and 20 mL (0.25 M) sodium selenosulphate. The total volume of the reaction mixture was made to 200 mL by adding double-distilled water. The beaker containing the reactive solution was transferred to an ice bath of 278 K temperature. The pH the resulting solution was found to be 9.5–10.5. Four clean glass slides were kept vertically enflaged on a specially designed substrate holder and rotated in the reaction mixture with a speed at 50 ± 2 rpm. The temperature of the solution was then allowed to rise slowly to 298 K. The substrates were removed from the beaker after 3 h. After the deposition, the substrates were taken from the bath, rinsed with distilled water, dried in air and kept in a dessicator.

A similar procedure was adapted to synthesis $Mo_{1-x}W_xSe_2$ thin films. The solutions of ammonium molybdate, sodium tungestate and sodium selenosulphate were mixed in the required stoichiometric ratio 1:1:2. The pH of the reactive solution was kept in the range 9.5–10.5.

---

* Corresponding author.
E-mail addresses: djsathe07@yahoo.co.uk (D.J. Sathe), pachate04@rediffmail.com (P.A. Chate).

0925-8388/$ – see front matter © 2010 Elsevier B.V. All rights reserved.
doi:10.1016/j.jallcom.2010.03.146

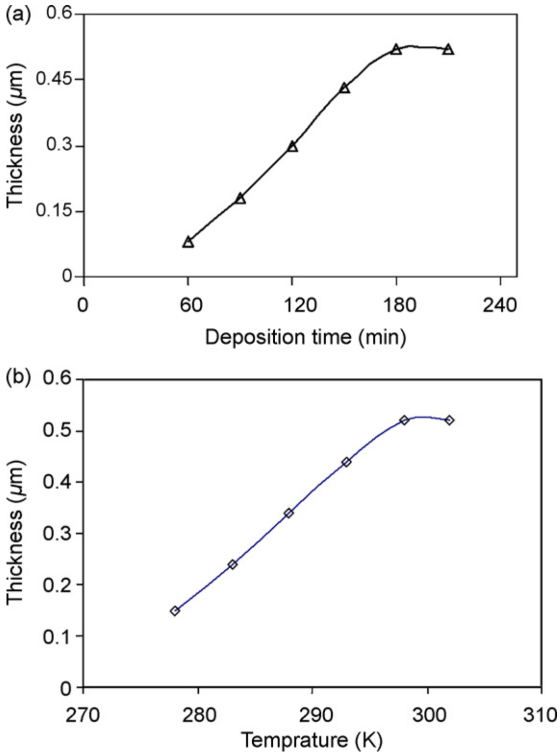

Fig. 1. (a) A plot of thickness vs. time for representative $Mo_{0.5}W_{0.5}Se_2$ thin film. (b) A plot of thickness vs. temperature for $Mo_{0.5}W_{0.5}Se_2$ thin film.

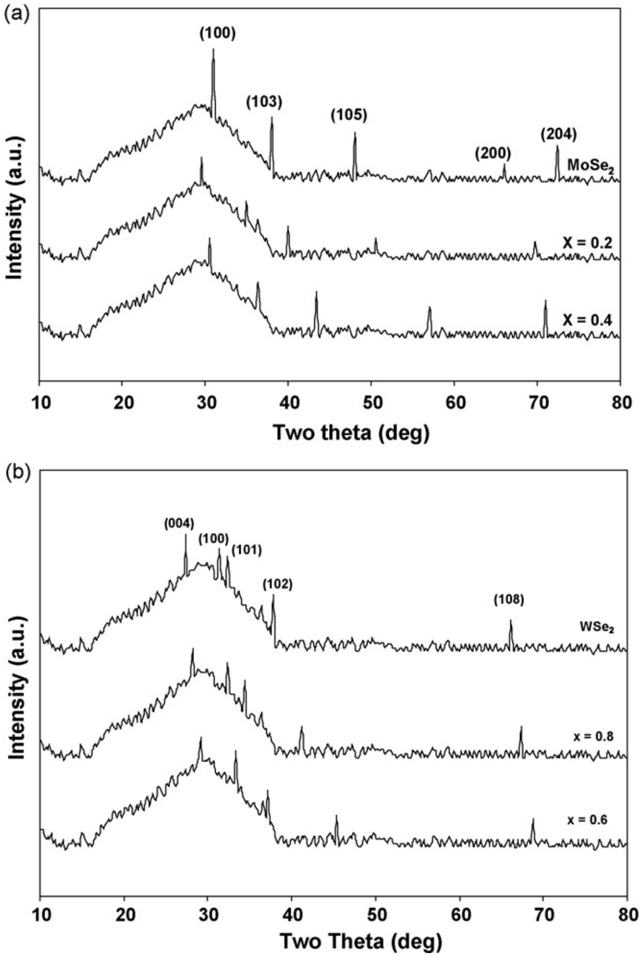

Fig. 2. XRD-pattern of $Mo_{1-x}W_xSe_2$ thin films; (a) ($x = 0.0$, 0.2, 0.4) (b) ($x = 0.6$, 0.8, 1.0).

3. Growth mechanism of $Mo_{1-x}W_xSe_2$ thin films

The rate of deposition of $Mo_{1-x}W_xSe_2$ film depends upon supersaturation, pH, composition of reactive species and temperature of bath. Initially reaction mixture is prepared by mixing ammonium molybdate, sodium tungestate, sodium selenosulphate and tartaric acid as complexing agent. Tartaric acid controls the metal ion concentration in the reaction vessel. Hydrazine hydrate acts as a reducing agent and it also serves complementary complex to help increase compactness and adherence of the film. A slow increase in temperature decomposes moderately stable sodium selenosulphate to yield Se^{2-}, while hydrazine hydrate reduce M^{6+} to M^{4+} in basic medium. The dissociation of M-TA complex at higher temperature liberates bear M^{4+} ions that react with Se^{2-} ion to get brown color thin film. The growth mechanism can be described from the following reactions;

$$M^{6+} + 3A^{2-} \rightarrow [M(A)_3] \qquad (M = Mo, W)$$

$$[M(A)_3] + 2NH_2\text{-}NH_2 + 2OH^- \rightarrow M^{4+} + 3A + 2H_2O + 2N_2\uparrow$$

$$Na_2SeSO_3 + OH^- \rightarrow Na_2SO_4 + HSe^-$$

$$HSe^- + OH^- \rightarrow H_2O + Se^{2-}$$

$$(1-x)[Mo(A)_3] + x[W(A)_3] + 2Se^{2-} \rightarrow Mo_{1-x}W_xSe_2 + 3A$$

In chemical bath deposition method, the ionic product exceeds the solubility product; precipitation take place and ions combine on the substrate and in the solution to form nuclei followed by growth process. The film deposition takes place by recombination of ions on the glass surface via nucleation followed by growth. The deposition of film occurs when the ionic product of M^{4+} and Se^{2-} exceeds the solubility product. In the growth process, no film formation occurs within first 60 min. This is the induction period required to from nucleation centers on the substrates. The presences of induction period suggest ion-by-ion growth mechanism instead of cluster-by-cluster.

The present investigation indicates that homogenous $Mo_{1-x}W_xSe_2$ films have been deposited at 180 min. The thickness was measured every 30 min and plotted against time as shown in Fig. 1(a). From the figure, the thickness varies linearly with time, but above 180 min the concentration of the reactive species decreases and results in decrease in thickness. All the films were homogenous well adherent to the substrate. Growth kinetics for the development of typical $Mo_{0.5}W_{0.5}Se_2$ films is shown in Fig. 1(b) 50 ± 2 rpm rotation speed was selected to deposit $Mo_{1-x}W_xSe_2$ thin films. The optimum condition in the deposition process for yielding good quality deposits are 298 K deposition temperature and 180 min deposition time. The films obtained were well adherent and of brown color.

4. Sample characterization

Crystallographic studies of films were characterized by using a Phillips PW-1710 X-ray diffractometer with Cu Kα1 line ($\lambda = 1.54056$ Å) in 2θ range from 10° to 80°. The optical properties were studied by taking absorption spectra of films using a Hitachi-330 (Japan) double-beam spectrophotometer in the range from 400 to 900 nm at room temperature. A substrate absorption correction was made by placing an identical uncoated glass slides in the reference beam. A 250 MK-III, Stereoscan, Cambridge (UK) scanning electron microscope (SEM) was used for microstructural

Table 1
Crystallographic data of $Mo_{1-x}W_xSe_2$ thin film.

Film compositions	Observed ‘*d*’ (Å)	Standard ‘*d*’ of $MoSe_2$ (Å)	Standard ‘*d*’ of WSe_2 (Å)	*h k l* planes	Cell parameters (Å)	Crystallite sizes (Å)
$MoSe_2$	2.879	2.846		1 0 0	$a=b=3.281$ $c=12.882$	224
	2.366	2.368		1 0 3		
	1.895	1.909		1 0 5		
	1.415	1.422		2 0 0		
	1.303	1.303		2 0 4		
$Mo_{0.9}W_{0.1}Se_2$	2.8863	2.846		1 0 0	$a=b=3.284$ $c=12.893$	219
	2.4161	2.368		1 0 3		
	1.9951	1.909		1 0 5		
	1.5178	1.422		2 0 0		
	1.3137	1.303		2 0 4		
$Mo_{0.8}W_{0.2}Se_2$	2.9193	2.846		1 0 0	$a=b=3.289$ $c=12.905$	214
	2.4645	2.368		1 0 3		
	2.0821	1.909		1 0 5		
	1.6137	1.422		2 0 0		
	1.3245	1.303		2 0 4		
$Mo_{0.7}W_{0.3}Se_2$	2.9671	2.846		1 0 0	$a=b=3.292$ $c=12.914$	210
	2.5120	2.368		1 0 3		
	2.1680	1.909		1 0 5		
	1.7094	1.422		2 0 0		
	1.3352	1.303		2 0 4		
$Mo_{0.6}W_{0.4}Se_2$	3.0081	2.846		1 0 0	$a=b=3.298$ $c=12.917$	204
	2.5609	2.368		1 0 3		
	2.2534	1.909		1 0 5		
	1.8043	1.422		2 0 0		
	1.3456	1.303		2 0 4		
$Mo_{0.5}W_{0.5}Se_2$	3.0481	2.846		1 0 0	$a=b=3.303$ $c=12.929$	193
	2.612	2.368		1 0 3		
	2.3397	1.909		1 0 5		
	1.904	1.422		2 0 0		
	1.3567	1.303		2 0 4		
$Mo_{0.4}W_{0.6}Se_2$	3.0814		3.250	0 0 4	$a=b=3.307$ $c=12.942$	189
	2.6872		2.850	1 0 0		
	2.4257		2.770	1 0 1		
	1.9969		2.380	1 0 3		
	1.3678		1.410	1 0 8		
$Mo_{0.3}W_{0.7}Se_2$	3.1283		3.250	0 0 4	$a=b=3.311$ $c=12.952$	187
	2.7051		2.850	1 0 0		
	2.5117		2.770	1 0 1		
	2.0927		2.380	1 0 3		
	1.3779		1.410	1 0 8		
$Mo_{0.2}W_{0.8}Se_2$	3.1692		3.250	0 0 4	$a=b=3.317$ $c=12.966$	181
	2.7537		2.850	1 0 0		
	2.5979		2.770	1 0 1		
	2.1885		2.380	1 0 3		
	1.3887		1.410	1 0 8		
$Mo_{0.1}W_{0.9}Se_2$	3.2093		3.250	0 0 4	$a=b=3.321$ $c=12.976$	174
	2.8021		2.850	1 0 0		
	2.6839		2.770	1 0 1		
	2.2842		2.380	1 0 3		
	1.3991		1.410	1 0 8		
WSe_2	3.250		3.250	0 0 4	$a=b=3.325$ $c=13.00$	159
	2.851		2.850	1 0 0		
	2.775		2.770	1 0 1		
	2.382		2.380	1 0 3		
	1.413		1.410	1 0 8		

observations. The electrical resistance measurements were carried out in the temperature range 300–500 K on a Zintek 502 BC milliohm meter using the two-probe method. A quick drying silver paste was applied at the ends of the film for better ohmic contact. Maintaining a temperature gradient along the length of the film and measuring the potential difference across the terminals having a separation of 1 cm with the help of digital micro-voltmeter made thermoelectric power measurement. A calibrated thermocouple probe (chrome alumel) with a digital indicator was used to sense the working temperature.

5. Result and discussion

5.1. XRD studies

The XRD-pattern of films were obtained by using a Phillips PW-1710 X-ray diffractometer with Cu $K\alpha_1$ line ($\lambda = 1.54056$ Å) in 2θ range from 10° to 80°. The XRD-pattern of representative $Mo_{1-x}W_xSe_2$ thin films are shown in Fig. 2(a) ($x = 0.0, 0.2, 0.4$) and (b) ($x = 0.6, 0.8, 1.0$). The presence of a large number of peaks indicates that the films are polycrystalline in nature. The observed ‘*d*’

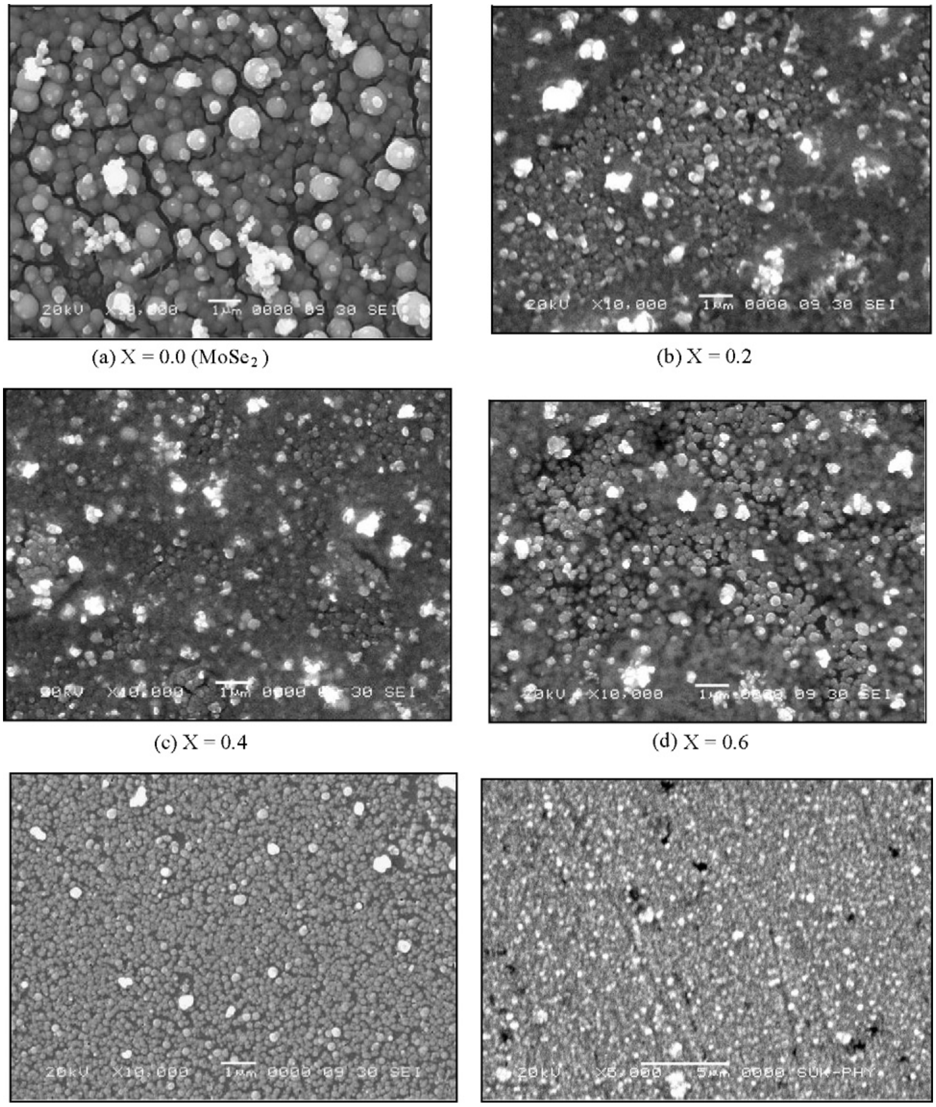

(a) X = 0.0 ($MoSe_2$) (b) X = 0.2

(c) X = 0.4 (d) X = 0.6

(e) X = 0.8 (f) X = 1.0 (WSe_2)

Fig. 3. SEM photographs of various $Mo_{1-x}W_xSe_2$ thin films ($x = 0.0$, 0.2, 0.4, 0.6, 0.8, 1.0).

values for deposited samples were in good agreement with the standard ‘*d*’ values taken from JCPDS diffraction file No. 15-0029 ($MoSe_2$)and JCPDS-06-0080 (WSe_2). Comparison of observed ‘*d*’ with standard ‘*d*’ values confirms that chemically deposited film shows of single phase compound with typical lines belonging to hexagonal structure in accordance with the literature reported data [4,16,20].

At the experimental conditions, $MoSe_2$ and $Mo_{1-x}W_xSe_2$ films with $0.0 < x \leq 0.5$ showed prominent peaks due to reflections from (1 0 0), (1 0 3), (1 0 5), (2 0 0) and (2 0 4) planes of a hexagonal $MoSe_2$ structure. A significant shift in peak position with changes in concentration was not observed and hence, it can be conjectured that addition of tungsten ions in $MoSe_2$ up to $x < 0.5$ forms alloy in the form of a solid solution. A small increase in lattice parameter is observed with the gradual addition of tungsten ions in $MoSe_2$ and is in conformity with the probable solid solution formation in terms of incorporation of tungsten ions in $MoSe_2$. Since the ionic radius of the tungsten ion is known to be slightly greater than the molybdenum ion, additions of tungsten ions in $MoSe_2$ gradually expand the cell uniformly. Although, the X-ray diffraction pattern shows a shift in diffraction line position, the number of lines is not altered, which gives an evidence that the cell symmetry is not changed by addition of tungsten. However, for higher values of x ($1.0 \leq x \leq 0.5$), the entire films exhibited highest intensity reflection peak at $d = 3.25$ Å (0 0 4). Along with (0 0 4) plane (1 0 0), (1 0 1), (1 0 3), (1 0 8) planes were peaks corresponding to hexagonal structure of WSe_2.A small increase in lattice parameter is observed with the gradual addition of tungsten ions in $MoSe_2$.which indicates that tungsten ions go into form solid solution with $MoSe_2$. The lattice parameters ‘*a* and *c*’ were found to be 3.28 Å and 12.882 Å for $MoSe_2$film and 3.325 Å 12.921 Å for WSe_2 respectively. The variation of the lattice parameters as a function of composition ‘*x*’ and the results show that the values of ‘*a*’ and ‘*c*’ vary linearly with ‘*x*’ following Vegard’s law [12]. The crystallite sizes of thin films were determined by using Scherrer formula and listed in Table 1.

5.2. Microscopic characterization

Scanning electron microscopy (SEM) is convenient technique to study the surface morphology of thin films. The SEM micrographs of $Mo_{1-x}W_xSe_2$ ($x = 0.0$, 0.2, 0.4, 0.6, 0.8, 1.0) thin films are shown in Fig. 3. All the thin films are homogenous, well cover to glass substrate and without any cracks or pinholes. The spherical grains are seen to be fused with adjacent. This type of morphology is typical of layered structure [19,21,22].

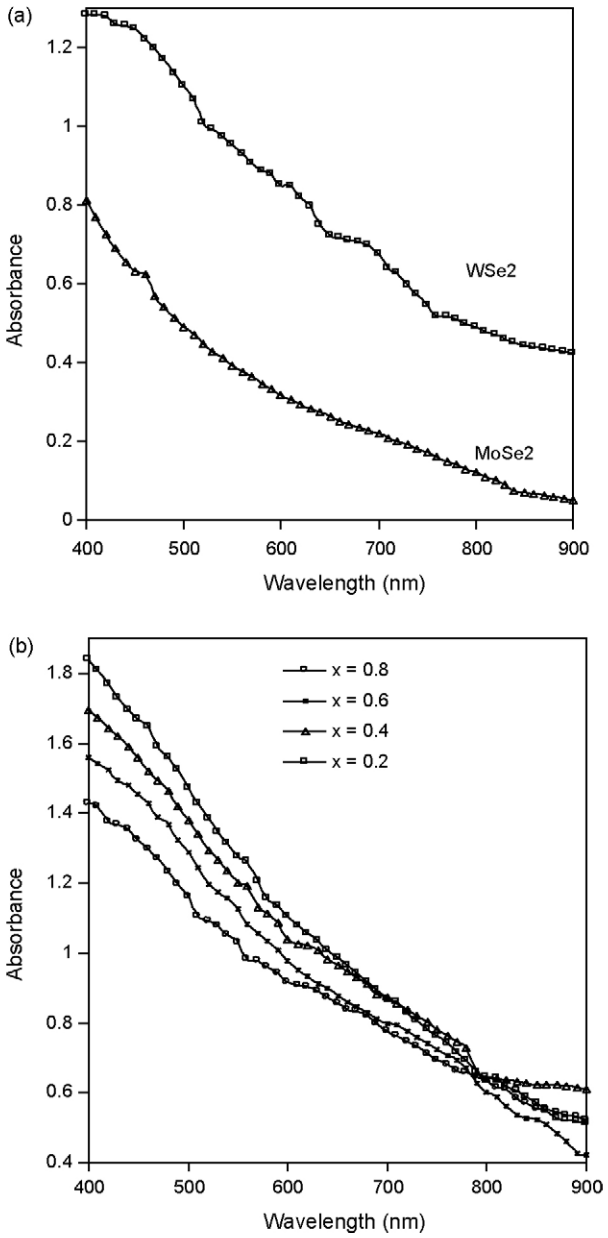

Fig. 4. Absorption spectra of $Mo_{1-x}W_xSe_2$ thin film samples (a) for films with $x = 0.0$, 0.1, (b) for films with $x = 0.2$, 0.4, 0.6, 0.8.

5.3. *Optical studies*

The optical absorption spectra for $Mo_{1-x}W_xSe_2$ films deposited onto a glass substrate were obtained in the wavelength range of 400–900 nm without considering losses due to reflection and transmission. Fig. 4(a) and (b) represents the absorption spectra of few representative samples. The optical absorption studies revealed a high absorption coefficient with allowed direct type of transition.

The interpretation of experimental results is most often performed with the help of the formula derived for a 3D crystal. The simplest form of the equation obeyed near and above the absorption edge is; [23]

$$\alpha h\nu = A(h\nu - E_g)^{1/2}$$

A plot of $(\alpha h\nu)^2$ versus $h\nu$ should be a straight line whose intercept to the x-axis gives the optical band gap. The graphs of $(\alpha h\nu)^2$ versus $h\nu$ for 'as deposited' samples are shown in Fig. 5(a) ($x = 0.0$, 0.2) (b) ($x = 0.4$, 0.6) and (c) ($x = 0.8$, 1.0) for samples. The band gaps for various compositions slightly increase from 1.43 to 1.48 eV with increase in mole fraction of tungsten (x).

5.4. *Electrical & thermo electrical properties*

The dark conductivity of all samples was measured by using two-probe method in temperature range of 300–525 K. The specific conductance at room temperature of $MoSe_2$ and WSe_2 were found to be of the order of 10^{-5} to $10^{-2} (\Omega\,cm)^{-1}$, respectively. The specific conductance increases for the ternary films with composition parameters 'x'. The values of specific conductance of different composition at 300 and 525 K are listed in Table 2

The conductivity of the samples increases with increase in temperature, showing semiconducting behavior of the films. The plot of $\log\sigma$ versus $1000/T$ is shown in Fig. 6(a and b). The plots are linear for $Mo_{1-x}W_xSe_2$ films indicating the presence of only one type of conduction mechanism in the films. The activation energies obtained from the slopes of straight lines of $\log\sigma$ versus $1000/T$ plots (Fig. 5) are included in Table 2. The values were found to be between 0.683 and 0.990 eV at high temperature and 0.005 and 0.064 eV low temperatures. The values are in well agreement with earlier reported values for $MoSe_2$ and WSe_2 thin films [24–27].

Thermoelectrical power measurement of all films shows similar behavior of increasing thermoelectric power with increasing temperature. The increase in thermoelectric power with temperature suggests the degenerate nature of the films. In thermoelectric power measurements, the open circuits thermovoltage generated by samples, when a temperature gradient is applied across 2-cm length of samples was measured. From the sign of terminal con-

Table 2
Electrical parameters of $Mo_{1-x}W_xSe_2$ thin film.

Sr. No.	Composition	Specific conductance $(\Omega\,cm)^{-1}$		Activation energy (eV)	
		At 300 K	At 525 K	HT	LT
01	$MoSe_2$	2.7×10^{-5}	5.45×10^{-3}	0.683	0.005
02	$Mo_{0.9}W_{0.1}Se_2$	3.25×10^{-5}	4.49×10^{-3}	0.706	0.016
03	$Mo_{0.8}W_{0.2}Se_2$	3.92×10^{-5}	3.58×10^{-3}	0.702	0.031
04	$Mo_{0.7}W_{0.3}Se_2$	4.14×10^{-5}	3.28×10^{-3}	0.741	0.041
05	$Mo_{0.6}W_{0.4}Se_2$	4.59×10^{-5}	8.46×10^{-3}	0.773	0.055
06	$Mo_{0.5}W_{0.5}Se_2$	8.33×10^{-5}	2.18×10^{-3}	0.797	0.162
07	$Mo_{0.4}W_{0.6}Se_2$	9.50×10^{-5}	5.32×10^{-3}	0.829	0.271
08	$Mo_{0.3}W_{0.7}Se_2$	7.14×10^{-5}	1.64×10^{-3}	0.858	0.382
09	$Mo_{0.2}W_{0.8}Se_2$	1.35×10^{-4}	5.62×10^{-2}	0.880	0.488
10	$Mo_{0.1}W_{0.9}Se_2$	6.25×10^{-3}	1.32×10^{-2}	0.912	0.593
11	WSe_2	1.58×10^{-2}	2.77×10^{-1}	0.99	0.640

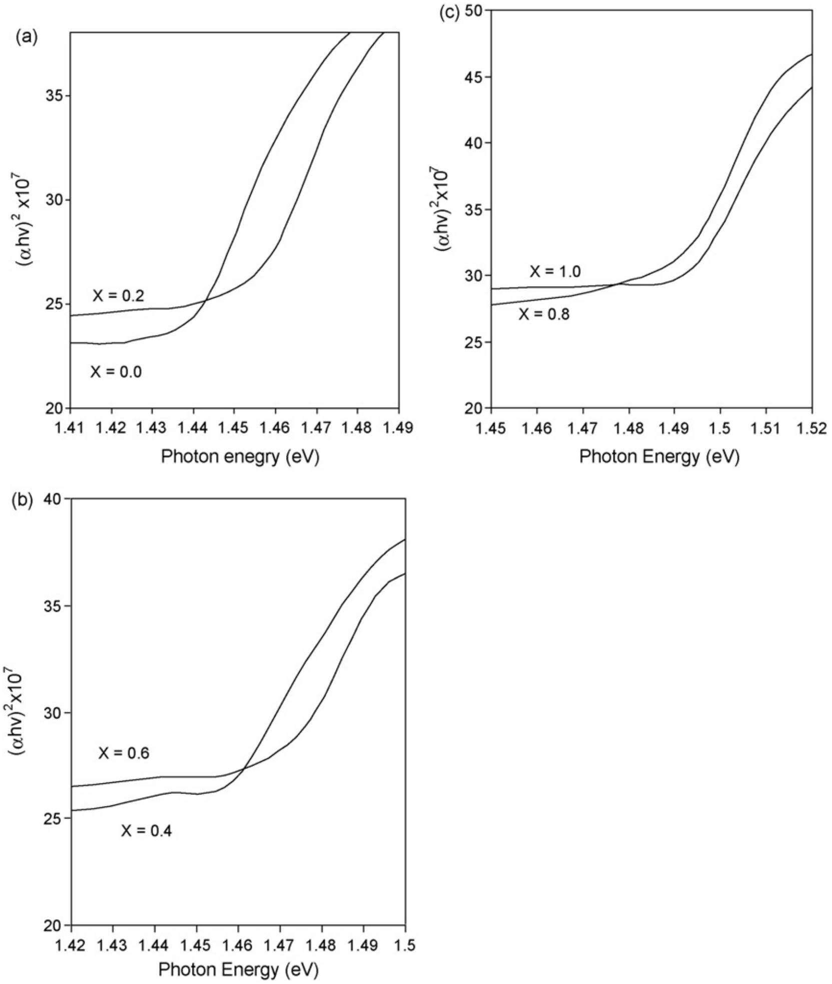

Fig. 5. Determination of band gap for $Mo_{1-x}W_xSe_2$ thin films.

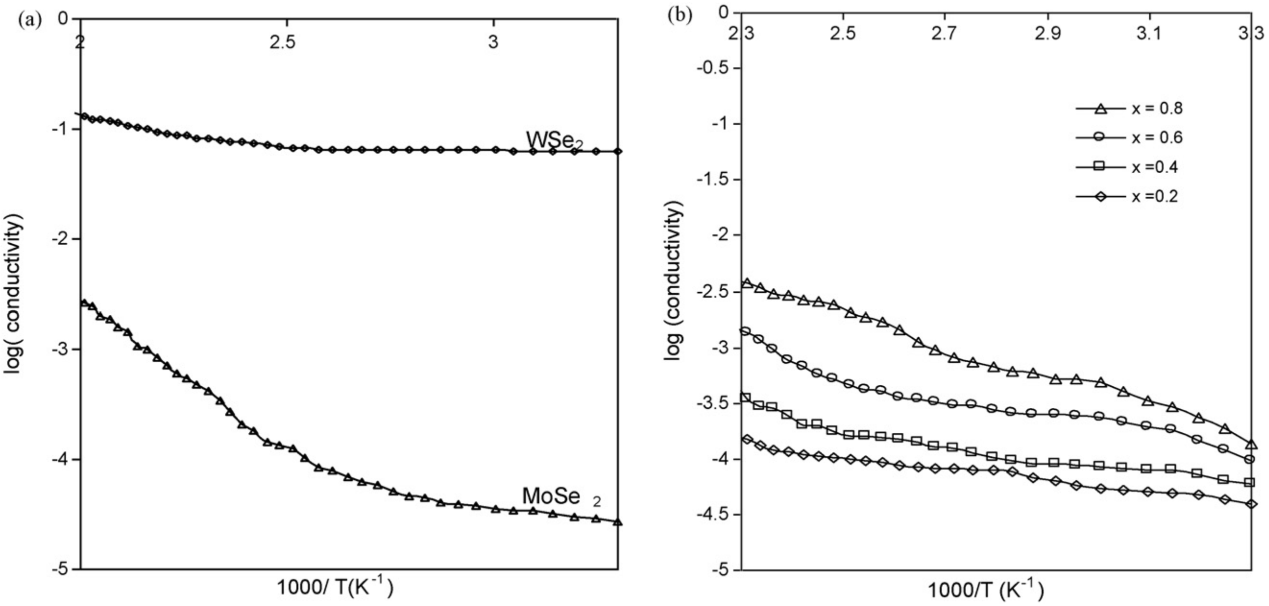

Fig. 6. A plot of ‘log σ’ with inverse of absolute temperature for $Mo_{1-x}W_xSe_2$ thin films $x = 0.1, 0.3, 0.5, 0.7, 0.9$.

nected to cold end of the sample, one can decide the sign of the predominant charge carrier [28]. In our study, the negative terminal was connected to cold end therefore all the film show n-type conductivity.

6. Conclusions

1. $Mo_{1-x}W_xSe_2$ can be deposited at low temperature by a modified chemical deposition technique.
2. The film formation takes place via nucleation and growth.
3. Crystallographic studies shows that $Mo_{1-x}W_xSe_2$ exist in hexagonal structure. As the composition parameter (x) increases, the '*d*' value, lattice parameter increases slightly.
4. Optical studies revealed the presence of direct band gap. The band gap value slightly increases.
5. The specific conduction at room temperature of $Mo_{1-x}W_xSe_2$ thin films were found to be of the order of 10^{-5} to $10^{-2} (\Omega\,\text{cm})^{-1}$.

References

[1] A. Jäger-Waldau, E. Bucher, Thin Solid Films 200 (1991) 157.
[2] M.K. Agarwal, H.B. Patel, K. Nagireddy, J. Cryst. Growth 41 (1977) 84.
[3] S. Mary Delphine, M. Jayachandran, C. Sanjeeviraja, Mater. Chem. Phys. 81 (2003) 78.
[4] J. Devadasan, C. Sanjeeviraja, M. Jayachandran, Mater. Chem Phys. 77 (2003) 397.
[5] O. Wisser, S. Landa, Catalysts, Their Properties & Application, Pergamon, Oxford, 1973.
[6] M.H. Whittingham, F. Levy (Eds.), Intercalated Layered Materials, Reidel, Dordrecht, 1979, p. 533.
[7] G. Prasad, O.N. Shrivastava, J. Phys. D: Appl. Phys. 21 (1988) 1028.
[8] G. Kline, K.K. Kam, D. Canfield, B.A. Parkinson, Solar Energy Mater. 4 (1980) 2471.
[9] H.D. Abruna, G.A. Hope, A.J. Bard, J. Electrochem. Soc. 29 (1982) 2224.
[10] K. Agarwal, V.V. Rao, Matter Sci. Lett. 9 (1996) 1023.
[11] R. Tenne, A. Woldm, Appl. Phys. Lett. 47 (1985) 707.
[12] M.K Agarwal, P.A. Wani, Mater. Res. Bull. 14 (1979) 825.
[13] M.K. Agarwal, P.A. Wani, P.D. Patel, J. Cryst. Growth 49 (1980) 693.
[14] M.K. Agarwal, L.T. Talell, Solid State Commun. 76 (1986) 549.
[15] M.K. Agarwal, M.N. Vashi, A.R. Jani, J. Cryst. Growth 71 (1985) 414.
[16] M.K. Agarwal, P.D. Patel, R.M. Joshi, J. Mater. Sci. Lett. 5 (1986) 66.
[17] W.K. Hofmann, H.J. Lewerern, C. Pettenkofer, Solar Energy Mater. 17 (1988) 165.
[18] G. Kline, K.K. Kam, R. Ziegler, B.A. Parkinson, Solar Energy Mater. 6 (1982) 337.
[19] P.P. Hankare, A.H. Manikshete, D.J. Sathe, P.A. Chate, K.C. Rathod, J. Mater. Chem. Phys. 113 (2009) 183.
[20] G Salitera, G. Hodes, E. Klein, R. Tenne, Thin Solid Films 245 (1994) 190.
[21] P.P. Hankare, A.H. Manikshete, D.J. Sathe, P.A. Chate, J. Mater. Sci.: Mater. Electron. 10854 (2009) 9980.
[22] P.P. Hankare, A.A. Patil, P.A. Chate, K.M. Garadkar, D.J. Sathe, A.H. Manikshete, I.S. Mulla, J. Cryst. Growth 311 (2008) 15.
[23] P.P. Hankare, P.A. Chate, D.J. Sathe, A.A. Patil, J. Mater. Sci.: Mater. Electron. 20 (2009) 776.
[24] P.P. Hankare, P.A. Chate, S.D. Delekar, V.M. Bhuse, M.R. Asabe, B.V. Jadhav, K.M. Garadkar, J. Cryst. Growth 291 (2006) 40.
[25] S. Mary Delphine, M. Jayachandran, C. Sanjeeviraja, Mater. Res. Bull. 40 (4) (2005) 135.
[26] J.C. Bernede, J. Pouzet, Z.K. Alaoui, Appl. Phys. A 51 (1990) 155.
[27] F. Fan, H. White, B.L. Wheeler, A.J. Bard, J. Electrochem. Soc. 127 (1980) 518.
[28] C.N. Rao, Modern Aspects of Solid state Chemistry, Plenum Press, New York, 1974.